Towards an objective edge detection algorithm based on discrete t-norms

M. González-Hidalgo[1] S. Massanet[1]

[1]Dept. of Math. and Comp. Science, University of the Balearic Islands, 07122 Palma de Mallorca, Spain

Abstract

In this paper a comparative analysis of different techniques in order to transform a gray-scale edge image to a thin binary edge image is performed. Several thresholding methods and thinning methods are compared. The comparison is made according to some performance measures, such as Pratt's figure of merit, Baddeley's measure and the ρ-coefficient. This study is an essential intermediate step to obtain an objective edge detection algorithm based on discrete t-norms. This fuzzy morphological algorithm has already shown notable potential in relation with the results obtained from nilpotent t-norms, umbra approach and classical edge detectors.

Keywords: Edge detection, discrete t-norm, mathematical morphology, thresholding method, thinning method.

1. Introduction

Edge detection is a fundamental low-level image processing operation, which is essential to carry out several higher level operations such as image segmentation, computer vision, motion and feature analysis and recognition. Its performance is crucial for the final results of the image processing techniques. A lot of edge detection algorithms have been developed over the last decades. These different approaches vary from the classical ones ([1]) based on a set of convolution masks, to the new techniques based on fuzzy sets ([2]).

Among the fuzzy approaches, the fuzzy mathematical morphology is a generalization of the binary morphology ([3]) using concepts and techniques from the fuzzy sets theory ([4], [5]). This theory allows a better treatment and a representation with greater flexibility of the uncertainty and ambiguity present in any level of an image. The morphological operators are the basic tools of this theory. A morphological operator P transforms an image A that one want to analyse into a new image $P(A, B)$ by means of an structuring element B. The four basic morphological operators are dilation, erosion, closing and opening. Thanks to the fact that gray-scale images can be represented as fuzzy sets, fuzzy tools can be used to define fuzzy morphological operators. Thus, conjuntors (usually continuous t-norms, but also uninorms, see [6]) and its residual implicators has been used.

However, gray-scale images are not represented in practice as functions of $\mathbb{R}^n$ into $[0, 1]$ because they are stored in finite matrices whose gray levels belong to a finite chain of 256 values. Therefore, the images are represented as discrete functions and discrete fuzzy operators can be used. In [7] and [8], the algebraic properties usually required to a morphology in order to become a "good" one were proved using discrete t-norms as conjunctors and their residual implicators. In both communications, some initial experimental results on edge detection were showed, improving, at least according to some performance measures, the results obtained by nilpotent t-norms, umbra approach and some classical edge detectors.

Usually the fuzzy edge image is an intermediate step before its binarization. The aim of this work is studying which is the best non-supervised way to make this transformation. Note that two processes must be analysed: binarization and obtention of edges of single pixel width. As a first approach, the binarization will be carried out through a single threshold. Thus, several thresholding methods will be compared. Thresholding is a simple but effective tool for classifying, according to the level of gray, the pixels into two types: those that belong to the background and those that belong to the object. The choice of best threshold is a difficult process and therefore, many methods exist in the literature to obtain it (see [9]). Here, the well-known Otsu's method (see [10]) and some fuzzy thresholding methods will be compared.

On the other hand, two methods will be compared to obtain thin edges. The first one, the non-maxima suppression (NMS) was proposed by Canny in [11]. He suggested that the NMS could be used as a post-processing operation along with the gradient operator for edge detection in order to obtain edges of single pixel width. The second one is the binary edge thinning algorithm of Zhang and Suen (see [12]). The main advantages of this algorithm is that it is fast and simple and it can be parallelized. Note, however that NMS acts on gray-scale edges while Zhang's algorithm, on binary edges. Thus, given a fuzzy edge image, two processes will be analysed: NMS and then a

thresholding method, or a thresholding method and then Zhang's algorithm. All these comparisons will be based on some objective performance measures vastly used in the edge detection literature: Pratt's figure of merit ([1]), Baddeley's measure ([13]) and the ρ-coefficient ([14]).

The communication is organized as follows. In Section 2, definitions and properties of fuzzy discrete morphological operators are recalled. In Section 3, the processes which will be compared are presented as well as the thresholding and thinning methods used in the following section. In addition, a brief description of the performance measures is presented. In Section 4 the obtained results are presented and analysed. Finally, some conclusions are pointed out.

2. Fuzzy discrete morphological operators

We will suppose the reader to be familiar with the basic definitions and properties of the fuzzy discrete logical operators that will be used in this work, specially those related to discrete t-norms and discrete residual implicators (see [15]). From now on, the following notation will be used: $L = \{0, \ldots, n\}$ a finite chain, $\mathcal{I}$ will denote a discrete implicator, $\mathcal{C}$ a discrete conjunctor, $\mathcal{N}$ the only strong negation on L which is given by $\mathcal{N}(x) = n - x$ for all $x \in L$, T a discrete t-norm, $\mathcal{I}_T$ its residual implicator, A a gray-scale image and B a gray-level structuring element that takes values on L.

Definition 1 *([7, 5]) The* fuzzy discrete dilation $D_{\mathcal{C}}(A, B)$ *and* the fuzzy discrete erosion $E_{\mathcal{I}}(A, B)$ *of A by B are the gray-scale images defined as*

$$\begin{aligned} D_{\mathcal{C}}(A,B)(y) &= \max_x \mathcal{C}(B(x-y), A(x)) \\ E_{\mathcal{I}}(A,B)(y) &= \min_x \mathcal{I}(B(x-y), A(x)). \end{aligned}$$

Definition 2 *([7, 5]) The* fuzzy discrete closing $C_{\mathcal{C},\mathcal{I}}(A, B)$ *and the* fuzzy discrete opening $O_{\mathcal{C},\mathcal{I}}(A, B)$ *of A by B are the gray-scale images defined as*

$$\begin{aligned} &C_{\mathcal{C},\mathcal{I}}(A,B)(y) = E_{\mathcal{I}}(D_{\mathcal{C}}(A,B), -B)(y) \\ &= \min_x \mathcal{I}(B(y-x), \max_z C(B(z-x), A(z))) \\ &O_{\mathcal{C},\mathcal{I}}(A,B)(y) = D_{\mathcal{C}}(E_{\mathcal{I}}(A,B), -B)(y) \\ &= \max_x C(B(y-x), \min_z \mathcal{I}(B(z-x), A(z))). \end{aligned}$$

The reflection $-B$ of an n-dimensional fuzzy set B is defined as $-B(x) = B(-x)$, for all $x \in \mathbb{Z}^n$.

Obviously a discrete t-norm is a conjunctor. Thus, these operators and their residual implicators can be used to define fuzzy discrete morphological operators using the previous definitions. In [7] and [8], the discrete t-norms that have to be used in order to preserve the morphological and algebraic properties that satisfy the classical morphological operators were fully determined. The most important algebraic properties of the fuzzy discrete morphological operators are monotonic properties, good interactions with Zadeh's union and intersection, generalized idempotence of the fuzzy closing and fuzzy opening. However, the key property in order to build an edge detector based on discrete t-norms is $E_{\mathcal{I}_T}(A, B) \subseteq A \subseteq D_T(A, B)$ when $B(0) = n$ and consequently, as in classical morphology, the difference between the fuzzy dilation and the fuzzy erosion of a gray-scale image,

$$D_T(A, B) \setminus E_{\mathcal{I}_T}(A, B),$$

called the *fuzzy gradient* operator, can be used in edge detection.

In addition to these properties, it is worth to safeguard the duality between the discrete fuzzy morphological operators. Therefore, discrete t-norms satisfying $\mathcal{I}_T = \mathcal{I}_{T,\mathcal{N}}$ are needed. This property holds for the discrete t-norms enumerated in the following result (see [16]).

Proposition 3 *The identity*

$$\mathcal{I}_T = \mathcal{I}_{T,\mathcal{N}}$$

is satisfied in the following cases:

1. *When T is the Łukasiewicz discrete t-norm,*

$$T_L(x, y) = \max\{0, x + y - n\}$$

2. *When T is the nilpotent minimum given by the following expression*

$$T_{nM}(x,y) = \begin{cases} 0 & \text{if } x + y \leq n \\ \min\{x, y\} & \text{otherwise} \end{cases}$$

3. *When T is an ordinal sum (with only one summand) of the Łukasiewicz t-norm in a square $[a, n-a]^2$, $a \in L$ with $a \leq n - a$, truncated by 0, given by the expression*

$$T_{nMa}(x,y) = \begin{cases} 0 & \text{if } x + y \leq n \\ x + y - (n-a) & \text{if } x + y > n \text{ and} \\ & a < x, y \leq n - a \\ \min\{x, y\} & \text{otherwise} \end{cases}$$

3. Algorithms of thinning and binarization

In the literature, there exist different approaches to edge detection based on fuzzy logic. These methods represent the edge image on a fuzzy way, i.e., they generate a image where each pixel value represents its membership to the edge set. Figure 1 is an example of these images. However, this idea contradicts the Canny restrictions ([11]). These restrictions force a representation of the edges as binary images with edges of one pixel wide.

Figure 1: Original image (left) and its fuzzy edge image (right)

In order to satisfy the Canny's restrictions, the fuzzy edge image has to be binarized and thinned. However, these two operations can be carried out in a different order. This is the essence of the two algorithms that will be analysed (see Figure 2).

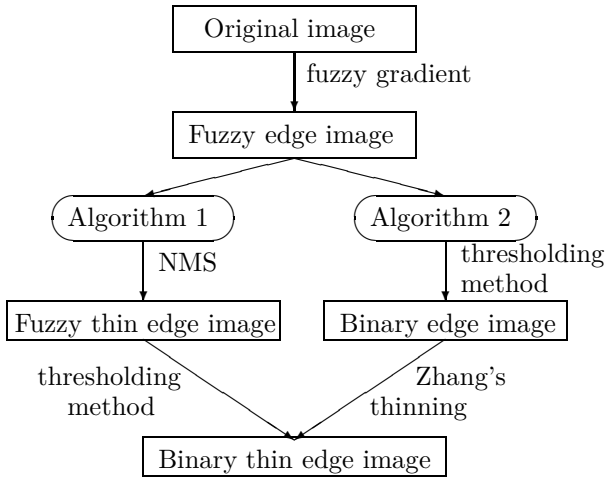

Figure 2: Block diagrams of the two algorithms considered.

Algorithm 1 consists on applying non-maxima suppression (NMS) to the fuzzy edge image in order to obtain edges of one pixel wide. The fuzzy edge image will contain large values where there is a strong image gradient, but to identify edges the broad regions present in areas where the slope is large must be thinned so that only the magnitudes at those points which are local maxima remain. NMS performs this by suppressing all values along the line of the gradient that are not peak values (see [11]). After that, a thresholding method is applied to binarize the fuzzy thin edges. On the other hand, Algorithm 2 performs a thresholding method at a first stage and then, a binary thinning algorithm is applied. In this case, we will use the well-known Zhang and Suen's algorithm (THIN) ([12]) because of its simplicity and speed.

As it is said above, a thresholding method must be applied in both algorithms. The following thresholding methods will be used:

- Otsu's method ([10]) that searches for the threshold that minimizes the intra-class variance, defined as a weighted sum of variances of the two resulting classes.
- Fuzzy C-means method, or FCM, ([17]), where fuzzy clustering memberships are assigned to pixels depending on their differences from the two class means.
- Thresholding using fuzzy measures, or FM, ([18]), where using an index of fuzziness, a similarity process is started to find the threshold point.
- Thresholding using Atanassov's intuitionistic fuzzy sets ([19]), where restricted dissimilarity functions are used in the construction of membership functions and the ambiguity is represented by means of Atanassov's intuitionistic fuzzy sets. Using two different dissimilarity functions and three different functions F to construct the fuzzy sets into the algorithm, six different algorithms are obtained. The dissimilarity functions are

  $$d_1(x,y) = |x-y|, \quad d_2(x,y) = \sqrt{|x^2-y^2|},$$

  and the used functions F, following [19], are

  $$\begin{array}{ll} F_1(x,y) & = 1 - 0.5x, \quad F_2(x,y) = \frac{1}{1+x}, \\ F_3(x,y) & = \exp(-x^2 \cdot \ln 2). \end{array}$$

3.1. Performance measures on edge detection

For the comparison of the obtained results, some performance measures have been considered. These measures need, in addition to the binary thin edge image (DE) obtained, a ground truth edge image (GT) that is a binary thin edge image containing the true edges of the original image, i.e., the reference edge image. There are several performance measures on edge detection in the literature (see [20]). In this work, we will use the following measures to quantify the similarity between (DE) and (GT):

1. Pratt's figure of merit ([1]) defined as $FoM =$

   $$= \frac{1}{\max\{card\{DE\}, card\{GT\}\}} \cdot \sum_{x \in DE} \frac{1}{1+ad^2},$$

   where *card* is the number of edge points of the image, a is a scaling constant and d is the separation distance of an actual edge point to the ideal edge points. In our case, we considered $a = 1$ and the Euclidean distance d.
2. The error metrics of Baddeley ([13]), inspired on Hausdorff distances is given by $\Delta_w^k(DE, GT) =$

   $$= \left[\frac{1}{|P|} \sum_{p \in P} |w(d(p, DE)) - w(d(p, GT))|^k \right]^{\frac{1}{k}},$$

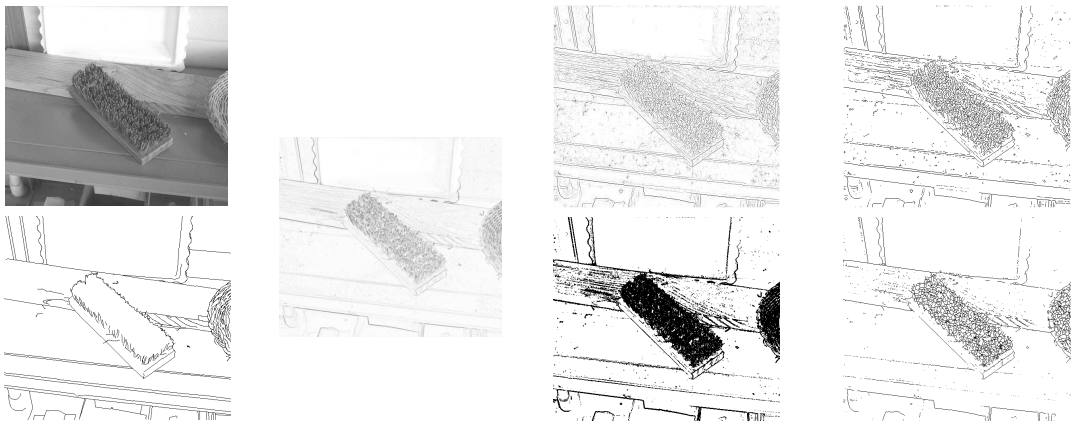

Figure 3: From left to right: original image and its ground truth; fuzzy edge image; Algorithm 1 (top) with fuzzy thin edge image (using NMS) and the final result (using Atanassov's d_2 and F_3) and Algorithm 2 (down) with binary edge image (using Atanassov's d_2 and F_1) and the final result (using Zhang's thinning).

Table 1: Results obtained

		Mean			St. deviation			% best results			% worst results		
Step 1	**Step 2**	*FoM*	Δ	ρ	*FoM*	Δ	ρ	*FoM*	Δ	ρ	*FoM*	Δ	ρ
NMS	Otsu	0.2619	33.085	0.422	0.0964	19.194	0.1491	0	0	0	0	0	0
	FM	0.2703	33.069	0.4289	0.0997	20.233	0.1516	12	12	18	0	0	0
	FCM	0.2643	32.907	0.425	0.0993	19.269	0.1526	2	2	2	0	0	0
	Ata11	0.1905	36.754	0.3125	0.0892	19.393	0.1478	0	0	0	0	0	0
	Ata12	0.1758	37.317	0.2889	0.0815	19.287	0.1367	0	0	0	76	88	98
	Ata13	0.2603	33.129	0.4196	0.0973	19.227	0.1506	0	0	0	0	0	0
	Ata21	0.2097	35.707	0.3423	0.1016	19.562	0.1642	0	0	0	0	0	0
	Ata22	0.1855	37.072	0.2998	0.0945	19.312	0.1412	0	0	0	0	2	2
	Ata23	0.3486	27.718	0.5297	0.112	17.059	0.1562	10	4	24	0	0	0
Otsu	THIN	0.3789	21.885	0.5223	0.1352	14.886	0.1671	20	14	22	0	0	0
FM		0.2571	31.352	0.3966	0.1276	20.885	0.1746	4	2	4	8	6	10
FCM		0.3748	23.05	0.519	0.1369	14.761	0.1687	22	20	8	0	0	0
Ata11		0.3168	27.08	0.47	0.1387	16.183	0.1828	2	6	4	2	0	2
Ata12		0.3041	27.6	0.4571	0.1388	16.187	0.185	4	0	4	6	0	2
Ata13		0.3784	22.725	0.5219	0.136	14.707	0.1675	16	10	12	0	0	0
Ata21		0.3353	26.462	0.4877	0.1481	15.9	0.189	10	8	8	0	0	2
Ata22		0.3115	27.448	0.463	0.1446	15.652	0.1895	4	4	4	6	0	2
Ata23		0.3426	22.759	0.4808	0.1218	14.852	0.1641	22	38	16	4	6	8

where P is the set of all the pixels of the image, $k \in \mathbb{R}$, $k > 0$, $d(p, A)$ represents the distance between the position p and the nearest position p' of A such that p' is an edge of A and $w : \mathbb{R} \to \mathbb{R}$ is any concave function. In our case, we considered $k = 2$, the Euclidean distance d and w, the identity function.

3. The ρ-coefficient ([14]), defined as

$$\rho = \frac{card(E)}{card(E) + card(E_{FN}) + card(E_{FP})},$$

where E is the set of well-detected edge pixels, E_{FN} is the set of ground truth edges missed by the edge detector and E_{FP} is the set of edge pixels detected but with no counterpart on the ground truth image.

4. Results and Analysis

As we have already observed, the performance measures need a dataset of images with their ground truth edge images (edges specifications) in order to compare the outputs obtained by the different algorithms. So, the images and their edge specifications from the public dataset of the University of South Florida[1] ([21]) have been used. This image dataset includes 50 natural images with their ground truth edge images. Each of the fifty images representing the domain of generic object recognition contains a single object approximately centered in the image, appearing unoccluded and set against a natural background for the object. The image dataset

[1]This image dataset can be downloaded from ftp://figment.csee.usf.edu/pub/ROC/edge_comparison_dataset.tar.gz

Figure 4: Original image (left) and its binary thin edge image (right) using Algorithm 2 with the Otsu's method.

contains indoor (39) and outdoor (11) scenes, and natural (8) and man-made (42) objects. Some images have highlights, reflections or low resolution.

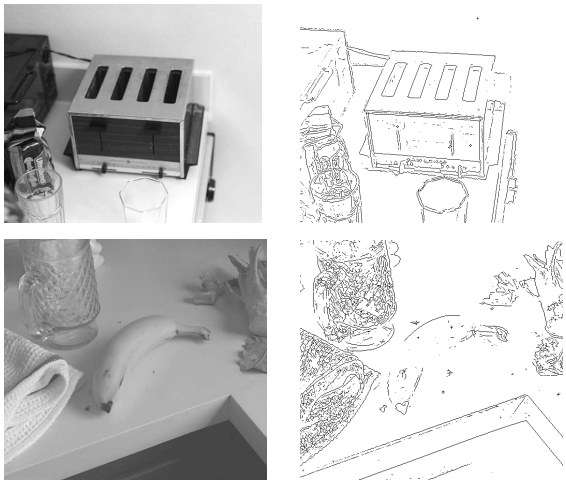

Figure 5: Original image (left) and its binary thin edge image (right) using Algorithm 1 with Atanassov's method with d_2 and F_3.

First of all, the fuzzy gradient operator is applied to the original image in order to obtain the fuzzy edge image. In the displayed experiments, the nilpotent minimum T_{nM} as conjunctor and the following structuring element

$$B = \begin{pmatrix} 0 & 255 & 0 \\ 255 & 255 & 255 \\ 0 & 255 & 0 \end{pmatrix}$$

are applied to obtain the dilation and the erosion of the image. After that, Algorithm 1 and Algorithm 2 with each thresholding method considered

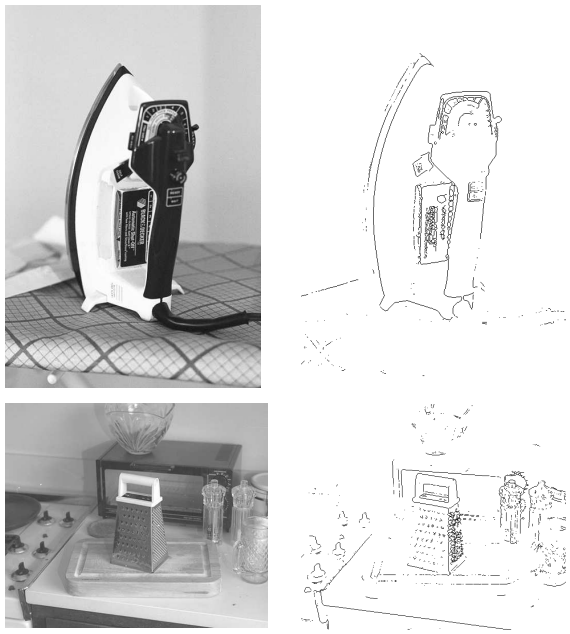

Figure 6: Original image (left) and its binary thin edge image (right) using Algorithm 2 with Atanassov's method taking d_2 and F_3.

are applied. Thus, a binary thin edge image is obtained and using the three performance measures, its similarity with the ground truth edge image is computed. In Figure 3, we show all the steps of an experiment using the two algorithms, applied to the original image displayed at the upper right corner that is the image 221 of the dataset.

Note that in this case, Algorithm 1 provides a better result than Algorithm 2 since the edges of the brush are more detailed in the first case and the shapes are better preserved. In order to make a general analysis, Table 1 shows the mean and the standard deviation for the three performance measures using all the configurations of the two algorithms. In addition, for a particular configuration of one algorithm, we specify the percentage of images for which this configuration is the best one or the worst one of the eighteen methods studied. In this table, Ataij means the Atanassov's thresholding method using d_i and F_j, respectively.

4.1. Performance measures and comparison of the methods

At a first sight, it is remarkable that the three performance measures do not point out the same algorithm as the best one. While Pratt's figure of merit and Baddeley's metric indicates that Algorithm 2 with the Otsu's method gives the best results on average, the ρ-coefficient shows that Algorithm 1 with Atanassov's method using d_2 and F_3 performs better than the other ones.

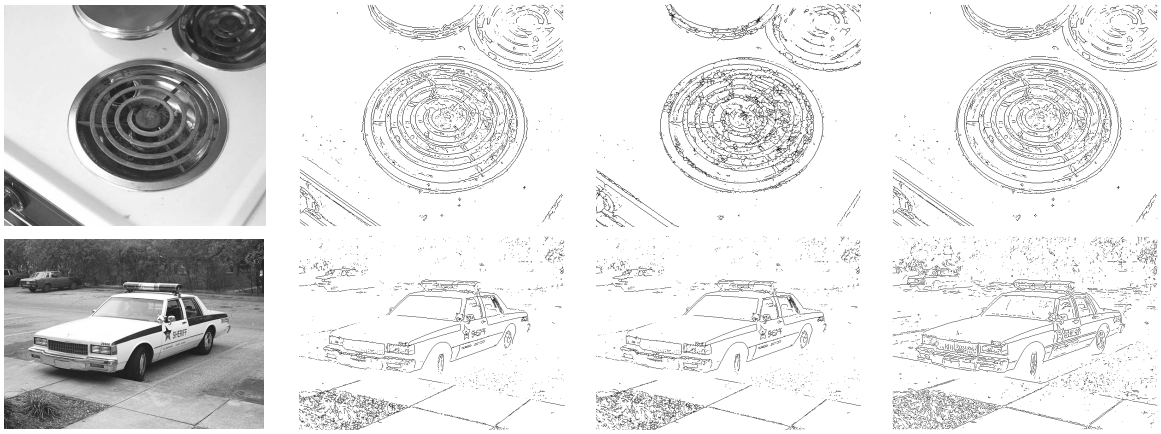

Figure 7: Original image (left) and the three best binary thin edge images according to FoM (2nd column), Baddeley (3rd) and ρ (4th). In the first row, from left to right and from top to down, Algorithm 1 with Ata23 is used for the images 2, 4 and 8, Algorithm 2 with Ata11 for image 3 and Algorithm 2 with Ata23 for images 6 and 7.

Figures 4 and 5 show the best results obtained for the displayed original images according to FoM and Baddeley's metric, and ρ-coefficient, respectively. In Figure 4, we have used Algorithm 2 with the Otsu's method and in Figure 5 the results are obtained using Algorithm 1 with Atanassov's method taking d_2 and F_3.

For the case of FoM and Baddeley's metric, note that the method with the best average marks is not the same with the largest percentage of best results. Algorithm 2 with Atanassov's thresholding method with d_2 and F_3 provides more often the best results according to these two performance measures, but on the other hand, it is the worst configuration for other images. Some examples can be seen in Figure 6. In general, the visualization of the results ensures this fact. Therefore, looking for a compromise between maximizing the percentage of best results and minimizing, as far as possible, the percentage of bad results, it is advisable to use Algorithm 2 with the Otsu's method to obtain more regular results.

The results also indicate that Algorithm 2 provides better results than Algorithm 1. In general, most configurations of Algorithm 1 detect too much "short edges" corresponding to illumination changes, textures and gray-scale variations inside objects. It is obvious that this fact could be avoided with a pre-processing step introducing a threshold related to the maximum length of an edge. However, there is no guarantee that the performance measures will improve and there is also the problem of determining this threshold. On the other hand, when the performance measures do not agree between the two algorithms, usually the one choosing Algorithm 1 provides a better result. In these cases, Algorithm 1 preserves edges better and they are better defined while Algorithm 2 tends to lose the continuity of some edges as we display in Figure 7. In addition, Algorithm 1 with FM method is the best configuration when we have an image with lots of texture. This fact can be seen in Figure 8.

Figure 8: Original image (left) and its binary thin edge image (right) with Algorithm 1 with fuzzy measures method.

One of the most important facts that can be extracted from the comparison of the results is the correlation of the best result obtained according to each performance measure and the visual perception of an observer. As it was already said, the three performance measures do not agree in general and they usually choose different methods as the best configuration for the same image. Comparing the best results obtained for the three measures, in more than fifty percent of the images Baddeley's metric provides the worst of the best results. This performance measure often gives better marks to low thresholds generating edge images with few edges. This fact can be observed in Figure 9 where the best result according to each performance

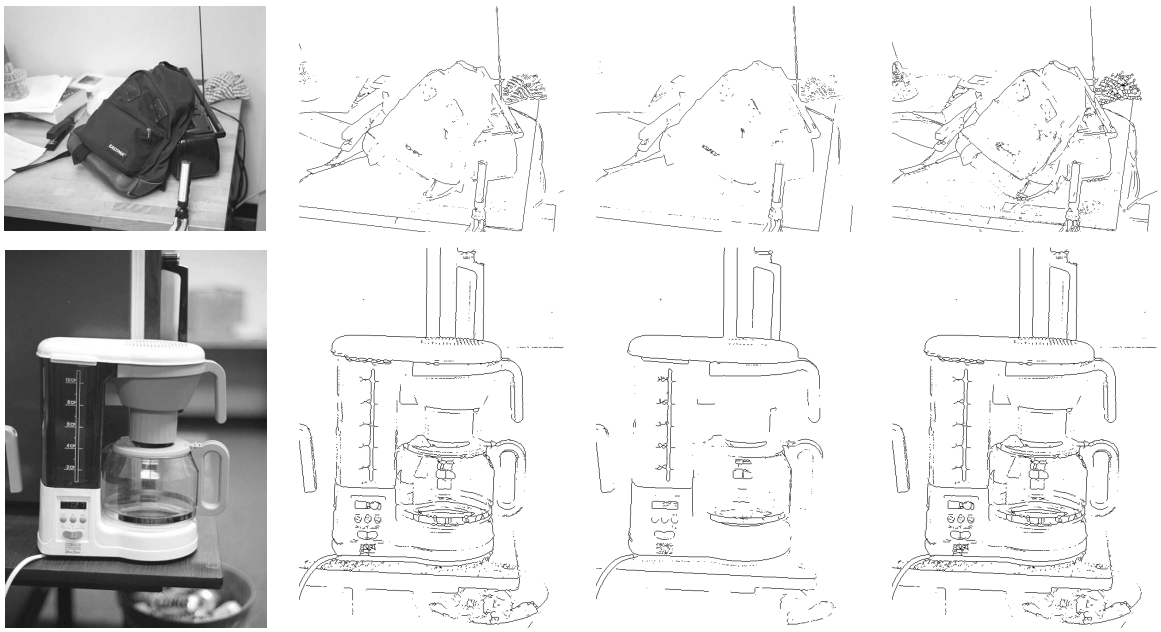

Figure 9: Original image (left) and the three best binary thin edge images according to FoM (2nd column), Baddeley (3rd) and ρ (4th).

measure is showed and the most simplified edge image is the corresponding one to the Baddeley's metric.

In order to check the goodness of the thresholding methods applied in this work, we have computed the best threshold for each image and each performance measure. The computation has been made in two ways. The first one, applying NMS and then determining the best threshold for each performance measure. The other one, for each possible threshold, we applied THIN and after that, we determined the best one for each performance measure. The results obtained are showed in Table 2. The first row indicates the best values for Algorithms 1 and 2. In the second row, we can see the values corresponding to the computed best threshold. Finally, in the second column % NMS-% THIN means the balance of the percentage of best results obtained applying NMS or THIN, respectively.

Analysing Table 2, we can observe that the thresholding methods employed do not find the computed best threshold according to the performance measures. Only three of the fifty images give the same result using Algorithms 1 or 2 than searching the best threshold. Another remarkable fact is that the percentage of best results using NMS increases drastically when we compute the best threshold. Finally, although the performance measure that is most improved in percentage is Baddeley's metric, the tendency that was observed initially with Algorithms 1 and 2 (edge images with few edges) increases exponentially searching the best threshold. Just note in Figure 10 how the police car of Figure 7 or the bag of Figure 9 have almost disappeared.

Figure 10: Best edge images according to Baddeley's metric searching the best threshold.

5. Conclusions

In this paper, we have tested several algorithms and thresholding methods in order to obtain a binary thin edge image, according to the Canny's criteria, from a fuzzy edge image. Considering the experimental results we can say that, in general terms, FoM and ρ-coefficient provide better results than Baddeley's metric. This performance measure generates edge images with few edges where important details are lost. From this, we could say that in our framework, the Baddeley's metric is not suitable. Moreover, several remarks can be made. Algorithm 2 with the Otsu's method should be used in order to obtain more regular results using FoM. In the case of ρ-coefficient the experimental results lead us to use Algorithm 1 with Ata23. In images with lots of texture the best performance measure is achieved using Algorithm 1 with FM. In these cases, the set of images of best results are complementary. After results analysis, we can conclude that the choice

Table 2: Results obtained searching the best threshold

Algorithm	Mean			% NMS - % THIN			% of improvement		
	FoM	Δ	ρ	FoM	Δ	ρ	FoM	Δ	ρ
Best 1 and 2	0.4213	18.875	0.5764	24-76	18-81	44-56	-	-	-
Best threshold	0.4832	13.871	0.6271	32-68	64-36	54-46	14.691	26.514	8.7913

of one of the two performance measures as well as the algorithm for edge detection is a personal issue depending on the accuracy of the visual results because the two algorithms present a higher performance for a large number of tested images.

Acknowledgment

This paper has been partially supported by the Spanish Grant MTM2009-10320 with FEDER support.

References

[1] W. K. Pratt. *Digital Image Processing*. Wiley-Interscience, 4 edition, February 2007.

[2] H. Bustince, E. Barrenechea, M. Pagola, and J. Fernandez. Interval-valued fuzzy sets constructed from matrices: Application to edge detection. *Fuzzy Sets Syst.*, 160(13):1819–1840, 2009.

[3] J. Serra. *Image analysis and mathematical morphology, vols. 1, 2.* Academic Press, London, 1982,1988.

[4] I. Bloch and H. Maître. Fuzzy mathematical morphologies: a comparative study. *Pattern Recognition*, 28:1341–1387, 1995.

[5] M. Nachtegael and E.E. Kerre. Classical and fuzzy approaches towards mathematical morphology. In Etienne E. Kerre and Mike Nachtegael, editors, *Fuzzy techniques in image processing*, number 52 in Studies in Fuzziness and Soft Computing, chapter 1, pages 3–57. Physica-Verlag, New York, 2000.

[6] M. González-Hidalgo, A. Mir-Torres, D. Ruiz-Aguilera, and J. Torrens. Image analysis applications of morphological operators based on uninorms. In *Proceedings of the IFSA-EUSFLAT 2009 Conference*, pages 630–635, Lisbon, Portugal, 2009.

[7] M. González-Hidalgo, S. Massanet, and J.Torrens. Discrete t-norms in a fuzzy mathematical morphology: Algebraic properties and experimental results. In *Proceedings of WCCI-FUZZ-IEEE*, pages 1194–1201, Barcelona, Spain, 2010.

[8] M. González-Hidalgo and S. Massanet. Closing and opening based on discrete t-norms. Applications to medical image analysis. Accepted in EUSFLAT-LFA 2011.

[9] M. Sezgin and B. Sankur. Survey over image thresholding techniques and quantitative performance evaluation. *J. Electronic Imaging*, 13(1):146–168, 2004.

[10] N. Otsu. A threshold selection method from gray-level histograms. *Systems, Man and Cybernetics, IEEE Transactions on*, 9:62–66, 1979.

[11] J. Canny. A computational approach to edge detection. *IEEE Trans. Pattern Anal. Mach. Intell.*, 8(6):679–698, November 1986.

[12] T. Y. Zhang and C. Y. Suen. A fast parallel algorithm for thinning digital patterns. *Commun. ACM*, 27:236–239, March 1984.

[13] A. J. Baddeley. An error metric for binary images. *Robust Computer Vision: Quality of Vision Algorithms*, pages 59–78, 1992.

[14] C. Grigorescu, N. Petkov, and M. A. Westenberg. Contour detection based on nonclassical receptive field inhibition. *IEEE Transactions on Image Processing*, 12(7):729–739, 2003.

[15] G. Mayor and J. Torrens. Triangular norms in discrete settings. In E.P. Klement and R. Mesiar, editors, *Logical, Algebraic, Analytic, and Probabilistic Aspects of Triangular Norms*, chapter 7, pages 189–230. Elsevier, Amsterdam, 2005.

[16] M. Mas, M. Monserrat, and J. Torrens. S-implications and R-implications on a finite chain. *Kybernetika*, 40:3–20, 2004.

[17] C. V. Jawahar, P. K. Biswas, and A. K. Ray. Investigations on fuzzy thresholding based on fuzzy clustering. *Pattern Recognition*, 30(10):1605 – 1613, 1997.

[18] N. V. Lopes, P. A. Mogadouro do Couto, H. Bustince Sola, and P. Melo-Pinto. Automatic histogram threshold using fuzzy measures. *IEEE Transactions on Image Processing*, 19(1):199–204, 2010.

[19] H. Bustince Sola, E. Barrenechea Tartas, M. Pagola, and R. Orduna. Image thresholding computation using Atanassov's intuitionistic fuzzy sets. *JACIII*, 11(2):187–194, 2007.

[20] G. Papari and N. Petkov. Edge and line oriented contour detection: State of the art. *Image and Vision Computing*, 29(2-3):79 – 103, 2011.

[21] K. Bowyer, C. Kranenburg, and S. Dougherty. Edge detector evaluation using empirical roc curves. *Computer Vision and Pattern Recognition*, 1:354–359, 1999.